Hindawi
Journal of Mathematics
Volume 2022, Article ID 2383074, 14 pages
https://doi.org/10.1155/2022/2383074

Research Article

Comparative Study of Y-Junction Nanotubes with Vertex-Edge Based Topological Descriptors

Al-Nashri Al-Hossain Ahmad

Department of Mathematics, Al Qunfudha University College, Umm Al-Qura University, Mecca, Saudi Arabia

Correspondence should be addressed to Al-Nashri Al-Hossain Ahmad; aanashri@uqu.edu.sa

Received 15 April 2022; Accepted 3 June 2022; Published 20 July 2022

Academic Editor: Muhammad Kamran Jamil

The current results of various forms of carbon nanostructures and its applications in different areas attract the researchers. In pharmaceutical, medicine, industry and electronic devices they used it by its graphical invariants. The detection of different types of carbon nanotubes junctions enhanced the attention and interest for forthcoming devices like transistors and amplifiers. A topological index plays a very important role in the study of physicochemical properties of biological and chemical structures. In this paper, we determine results of *ve*-degree topological indices for various type of carbon nanotubes Y-junctions and their comparisons. The particular indices called as The first *ve*-degree Zagreb β index, the second *ve*-degree Zagreb index, *ve*-degree Randic index, *ve*-degree atom-bond connectivity index, *ve*-degree geometric-arithmetic index, *ve*-degree harmonic index and *ve*-degree sum-connectivity index.

1. Introduction

Let a graph having vertex set V and edge set E possesses the properties of connectivity, usually labeled as $G = (V, E)$. For a vertex $x_1 \in V$, the concept of open neighborhood of that vertex x_1 is formulated as $N(x_1) = \{x_2 \in V: x_1x_2 \in E\}$, while the concept of closed neighborhood formulated and notated by $N[x_1] = N(x_1) \cup x_1$, [1–3]. A notation $\xi_{ve}(x_1)$, is used for the *ve*-degree of any vertex $x_1 \in V$, and measured by the count of distinct edges which are incident to any vertex from the closed neighborhood of x_1. Further detail and discussion on this notation and its mathematical definition, one can see [4–6].

In molecular graph theory, vertices and edges are replaced by atoms and their bonds while transforming from a molecular structure to a molecular graph, respectively, [7, 8]. Carbon nanotubes with branching ends are promising building blocks for next-generation enhanced nanoelectronics and nanodevices. In the junction family, three-terminal devices and carbon nanotube graphs have tremendous potential. While study the chemical things for various determinations in different areas, the energy bond is the one of the most important thermophysical to be measured. There are different type of nanotubes junctions for example, X, Y, L and T and their applications can be seen in [9–12].

The topological descriptor of a given graph is a numeric number that describes the quantitative structural-property relationship and quantitative structural-activity of the molecular graph [13–16]. The researcher in [17] discussed the metal-organic network, supramolecular chain is discussed by [18], carbon nanotubes are measured in [19] with different parameters of graph-based chemical theory. For study of different types of topological indices, see [20–25]. Some new variants and generalized results on the topological descriptors are found in the articles suggested [3, 26, 27].

There are variety of topological descriptors, one of them is the vertex-edge based that will be discussed in this article. The researchers in [1], defined the "*ev*-degree," and [4] contributed in this study. Basic definitions regarding "*ve*-degree" topological indices, refer to [28].

The vertex-edge based topological descriptors are: The first *ve*-degree Zagreb β index $(M^1_{\beta ve}(Y_m(n,n)) = \sum_{x_1x_2\in E} (\xi_{ve}(x_1) + \xi_{ve}(x_2)))$, the second *ve*-degree Zagreb index

$(M^2_{ve}(Y_m(n,n)) = \sum_{x_1x_2\in E}(\xi_{ve}(x_1)\times\xi_{ve}(x_2)))$, *ve*-degree Randić index $(R_{ve}(Y_m(n,n)) = \sum_{x_1x_2\in E}(\xi_{ve}(x_1)\times\xi_{ve}(x_2))^{(-1/2)})$, *ve*-degree atom-bond connectivity index $(ABC_{ve}(Y_m(n,n)) = \sum_{x_1x_2}\in E((\xi_{ve}(x_1)+\xi_{ve}(x_2)-2)/(\xi_{ve}(x_1)\times\xi_{ve}(x_2)))^{(1/2)})$, *ve*-degree geometric-arithmetic index $(GA_{ve}(Y_m(n,n)) = \sum_{x_1x_2\in E}((2(\xi_{ve}(x_1)\times\xi_{ve}(x_2))^{(1/2)})/(\xi_{ve}(x_1)+\xi_{ve}(x_2))))$, *ve*-degree harmonic index $(H_{ve}(Y_m(n,n)) = \sum_{x_1x_2\in E}(2/(\xi_{ve}(x_1)+\xi_{ve}(x_2))))$ and *ve*-degree sum-connectivity index $(\chi_{ve}(Y_m(n,n)) = \sum_{x_1x_2\in E}(\xi_{ve}(x_1)+\xi_{ve}(x_2))^{(-1/2)})$. For further results and detail on vertex-edge based topological indices see [29, 30]. Some other related topics based on the information of edges of a graph are detailed in [31–37]. In this paper, the exact values of vertex-edge based topological indices for Y-junctions carbon nanotubes are determined.

2. *Y*-Junction Graphs

The *Y*-junctions investigated in this paper are formed by the covalent interconnection of three finite-length armchair single-walled nanotubes that intersect at a 120° angle and are specified by the chiral vector (n,n). For detail study of structures, authors refer to [38–41]. A *Y*-junction graph is defined as follows:

Let n is even and m,n are two integers. A graph of *Y*-junction labeled as $Y_m(n,n)$ is constructed by using an armchair $Y(n,n)$, and three $CNTsT_m(n,n)$ single-walled armchair which are identical having m hexagons-layers. Total face count is $(3n^2/4)-(3n/2)+5$ in an armchair $Y(n,n)$, containing openings of count three, heptagons count is six, hexagons count is $(3n^2/4)-(3n/2)-5$. Furthermore, each armchair tube labeled by $T_m(n,n)$ contained hexagonal-faces of count $2mn$. The degree two count vertices are $6n$, degree three with count $(3n^2/2)+3n+12mn+6$, collectively having $(3n^2/2)+9n+12mn+6$ order, and $(9n^2/4)+(21n/2)+18mn+9$ size.

In this work, a junction graph labeled with $Y_m(n,n)$ is graphs having no pendent or degree one vertex, exists. This work also consists of other three topologies of *Y*-junction graphs labeled with $Y^1_m(n,n), Y^2_m(n,n)$ and $Y^3_m(n,n)$ and these contained some vertices with degree one. These further topologies are constructed by $Y_m(n,n)$-junction graphs by adding pendants to degree 2 vertices. Single tube among three tubes of $Y_m(n,n)$ has exactly $2n$ count of vertices having two degree. In result, $6n$ is the maximum number of pendants that can be utilised with this attachment for $Y_m(n,n)$ and $2n$ for each tube.

3. The *ve*-Degree Results of *Y*-Junction Graph $Y_m(n,n)$

This section presented the *ve*-degree results of *Y*-junction graph $Y_m(n,n)$. This graph does not contain any pendent vertex that is shown in Figure 1. The edge partition of end vertices *ve*-degree of each edge along with the degree of end vertices of each edge for $Y_m(n,n)$ graph is given in Table 1.

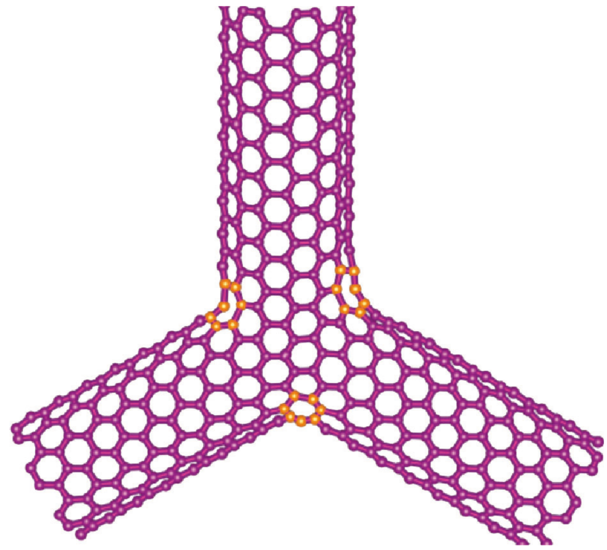

Figure 1: A variant of *Y*-junction $Y_m(n,n)$.

Table 1: The *ve*-degrees of each edge of $Y_m(n,n)$ junction graph.

$(\xi(x_1),\xi(x_2))$	$(\xi_{ve}(x_1),\xi_{ve}(x_2))$	Count
(2, 2)	(5, 5)	$3n$
(2, 3)	(5, 8)	$6n$
(3, 3)	(8, 9)	$6n$
(3, 3)	(9, 9)	$(9n^2/4)-(9n/2)+18mn+9$

3.1. The First ve-Degree Zagreb β Index.

$$\begin{aligned} M^1_{\beta ve}(Y_m(n,n)) &= \sum_{x_1x_2\in E}(\xi_{ve}(x_1)+\xi_{ve}(x_2)) \\ &= (10)(3n)+(13)(6n)+(17)(6n) \\ &\quad +(18)\left(\frac{9n^2}{4}-\frac{9n}{2}+18mn+9\right) \\ &= \frac{81n^2}{2}+129n+324mn+162. \end{aligned} \tag{1}$$

3.2. The Second ve-Degree Zagreb Index.

$$\begin{aligned} M^2_{ve}(Y_m(n,n)) &= \sum_{x_1x_2\in E}(\xi_{ve}(x_1)\times\xi_{ve}(x_2)) \\ &= (25)(3n)+(40)(6n)+(72)(6n) \\ &\quad +(81)\left(\frac{9n^2}{4}-\frac{9n}{2}+18mn+9\right) \\ &= \frac{729n^2}{2}+\frac{765n}{2}+1458mn+729. \end{aligned} \tag{2}$$

3.3. The Randić Index Developed by ve-Degree Methodology. Utilizing the edge-partition details described in the Table 1, we measured the Randić index developed by *ve*-degree methodology:

$$\begin{aligned} R_{ve}(Y_m(n,n)) &= \sum_{x_1x_2\in E} (\xi_{ve}(x_1)\times\xi_{ve}(x_2))^{(-1/2)} \\ &= (25)^{(-1/2)}(3n) + (40)^{(-1/2)}(6n) + (72)^{(-1/2)}(6n) + (81)^{(-1/2)}\left(\frac{9n^2}{4} - \frac{9n}{2} + 18mn + 9\right) \\ &= \frac{n^2}{4} + \left(\frac{1}{10} + \frac{3\sqrt{10}}{10} + \frac{\sqrt{2}}{2} + 2m\right)n + 1. \end{aligned} \tag{3}$$

3.4. The Atom-Bond Connectivity Index Developed by ve-Degree Methodology. Utilizing the edge-partition details described in the Table 1, we measured the atom-bond connectivity index developed by *ve*-degree methodology:

$$\begin{aligned} ABC_{ve}(Y_m(n,n)) &= \sum_{x_1x_2\in E} \left(\frac{\xi_{ve}(x_1)+\xi_{ve}(x_2)-2}{\xi_{ve}(x_1)\times\xi_{ve}(x_2)}\right)^{(-1/2)} \\ &= (3n)\sqrt{\frac{8}{25}} + (6n)\sqrt{\frac{11}{40}} + (6n)\sqrt{\frac{15}{72}} + \left(\frac{9n^2}{4} - \frac{9n}{2} + 18mn + 9\right)\sqrt{\frac{16}{81}} \\ &= n^2 + \left(\frac{6\sqrt{2}}{5} + \frac{3\sqrt{110}}{10} + \frac{\sqrt{30}}{2} + 8m - 2\right)n + 4. \end{aligned} \tag{4}$$

3.5. The Geometric-Arithmetic Index Developed by ve-Degree Methodology. Utilizing the edge-partition details described in the Table 1, we measured the geometric-arithmetic index developed by *ve*-degree methodology:

$$\begin{aligned} GA_{ve}(Y_m(n,n)) &= \sum_{x_1x_2\in E}^{\left(\frac{2(\xi_{ve}(x_1)\times\xi_{ve}(x_2))^{(-1/2)}}{\xi_{ve}(x_1)+\xi_{ve}(x_2)}\right)} \\ &= (3n)\frac{(2)\sqrt{25}}{10} + (6n)\frac{(2)\sqrt{40}}{13} + (6n)\frac{(2)\sqrt{72}}{17} + \left(\frac{9n^2}{4} - \frac{9n}{2} + 18mn + 9\right)\frac{(2)\sqrt{81}}{18} \\ &= \frac{9n^2}{4} + \left(\frac{-3}{2} + \frac{24\sqrt{10}}{13} + \frac{72\sqrt{2}}{17} + 18m\right)n + 9. \end{aligned} \tag{5}$$

3.6. The Harmonic Index Developed by ve-Degree Methodology. Utilizing the edge-partition details described in the Table 1, we measured the harmonic index developed by *ve*-degree methodology:

$$\begin{aligned} H_{ve}(Y_m(n,n)) &= \sum_{x_1x_2\in E}^{\left(\frac{2}{\xi_{ve}(x_1)+\xi_{ve}(x_2)}\right)} \\ &= (3n)\frac{2}{10} + (6n)\frac{2}{13} + (6n)\frac{2}{17} + \left(\frac{9n^2}{4} - \frac{9n}{2} + 18mn + 9\right)\frac{2}{18} \\ &= \frac{n^2}{4} + \left(\frac{3821}{2210} + 2m\right)n + 1. \end{aligned} \tag{6}$$

3.7. The Sum-Connectivity Index Developed by ve-Degree Methodology. Utilizing the edge-partition details described in the Table 1, we measured the sum-connectivity index developed by *ve*-degree methodology:

$$\begin{aligned}\chi_{ve}(Y_m(n,n)) &= \sum_{x_1x_2\in E}(\xi_{ve}(x_1)+\xi_{ve}(x_2))^{(-1/2)}\\ &= (3n)\frac{1}{\sqrt{10}}+(6n)\frac{1}{\sqrt{13}}+(6n)\frac{1}{\sqrt{17}}+\left(\frac{9n^2}{4}-\frac{9n}{2}+18mn+9\right)\frac{1}{\sqrt{18}}\\ &= \frac{3\sqrt{2}n^2}{8}+\left(\frac{3\sqrt{10}}{10}+\frac{6\sqrt{13}}{13}+\frac{6\sqrt{17}}{17}+\frac{\sqrt{2}}{6}\left(\frac{-9}{2}+18m\right)\right)n+\frac{3\sqrt{2}}{2}.\end{aligned} \tag{7}$$

4. The *ve*-Degree Results of *Y*-Junction Graph $Y_m^1(n,n)$

By attaching the $2n$ pendants vertices with 2 degree vertices to any one tube of $Y_m(n,n)$ graph, we obtain a new graph, it is denoted by $Y_m^1(n,n)$, see Figure 2. The order and size of $Y_m^1(n,n)$ graph is $(3n^2/2)+11n+12mn+6$ and $(9n^2/4)+(25n/2)+18mn+9$, respectively. This section determinen the *ve*-degree results of Y-junction graph $Y_m^1(n,n)$. The edge partition of end vertices *ve*-degree of each edge along with the degree of end vertices of each edge for $Y_m^1(n,n)$ graph is given in Table 2.

4.1. The First ve-Degree Zagreb β Index.

$$\begin{aligned}M_{\beta ve}^1\left(Y_m^1(n,n)\right) &= \sum_{x_1x_2\in E}(\xi_{ve}(x_1)+\xi_{ve}(x_2))\\ &= (10)(2n)+(13)(4n)+(16)(2n)+(10)(2n)+(17)(4n)+(14)(n)+(18)+\left(\frac{9n^2}{4}-\frac{5n}{2}+18mn+9\right)\\ &= \frac{81n^2}{2}+(161+324m)n+162.\end{aligned} \tag{8}$$

4.2. The Second ve-Degree Zagreb Index.

$$\begin{aligned}M_{ve}^2\left(Y_m^1(n,n)\right) &= \sum_{x_1x_2\in E}(\xi_{ve}(x_1)\times\xi_{ve}(x_2)),\\ M_{ve}^2\left(Y_m^1(n,n)\right) &= (25)(2n)+(40)(4n)+(63)(2n)+(21)(2n)+(72)(4n)+(49)(n)+(81)+\left(\frac{9n^2}{4}-\frac{5n}{2}+18mn+9\right)\\ &= 729+\frac{729n^2}{4}+\left(\frac{1025}{2}+1458m\right)n.\end{aligned} \tag{9}$$

4.3. The Randić Index Developed by ve-Degree Methodology. Utilizing the edge-partition details described in the Table 2, we measured the Randić index developed by *ve*-degree methodology:

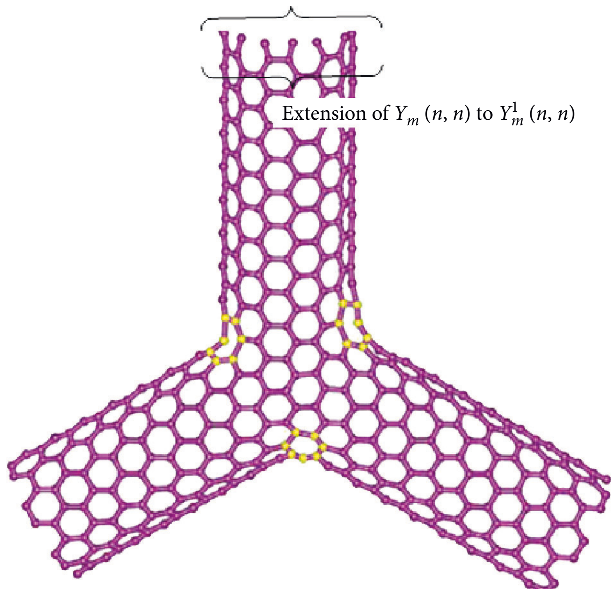

FIGURE 2: A variant of Y-junction $Y_m^1(n,n)$.

TABLE 2: The end vertices ve-degrees of each edge of $Y_m^1(n,n)$.

$(\xi(x_1),\xi(x_2))$	$(\xi_{ve}(x_1),\xi_{ve}(x_2))$	Count
$(2,2)$	$(5,5)$	$2n$
$(2,3)$	$(5,8)$	$4n$
$(3,3)$	$(7,9)$	$2n$
$(1,3)$	$(3,7)$	$2n$
$(2,3)$	$(8,9)$	$4n$
$(3,3)$	$(7,7)$	n
$(3,3)$	$(9,9)$	$(9n^2/4)-(5n/2)+18mn+9$

$$\begin{aligned} R_{ve}\left(Y_m^1(n,n)\right) &= \sum_{x_1x_2\in E}\left(\xi_{ve}(x_1)\times\xi_{ve}(x_2)\right)^{(-1/2)} \\ &= (35)^{(-1/2)}(2n)+(40)^{(-1/2)}(4n)+(63)^{(-1/2)}(2n)+(21)^{(-1/2)}(2n) \\ &\quad +(72)^{(-1/2)}(4n)+(49)^{(-1/2)}(n)+(81)^{(-1/2)}\left(\frac{9n^2}{4}-\frac{5n}{2}+18mn+9\right) \\ &= 1+\frac{n^2}{4}+\left(\frac{167}{630}+\frac{\sqrt{10}}{5}+\frac{2\sqrt{7}}{21}+\frac{2\sqrt{21}}{21}+\frac{\sqrt{2}}{3}+2m\right)n. \end{aligned} \tag{10}$$

4.4. The Atom-Bond Connectivity Index Developed by ve-Degree Methodology. Utilizing the edge-partition details described in the Table 2, we measured the atom-bond connectivity index developed by ve-degree methodology:

$$\begin{aligned}
ABC_{ve}\left(Y_m^1(n,n)\right) &= \sum_{x_1x_2\in E}\left(\frac{\xi_{ve}(x_1)+\xi_{ve}(x_2)-2}{\xi_{ve}(x_1)\times\xi_{ve}(x_2)}\right)^{(1/2)} \\
&= (2n)\sqrt{\frac{8}{25}}+(4n)\sqrt{\frac{11}{40}}+(2n)\sqrt{\frac{14}{63}}+(2n)\sqrt{\frac{8}{21}}+(4n)\sqrt{\frac{15}{72}}+(n)\sqrt{\frac{12}{49}}+\sqrt{\frac{16}{81}}\left(\frac{9n^2}{4}-\frac{5n}{2}+18mn+9\right) \\
&= 4+n^2+\left(\frac{22\sqrt{2}}{15}+\frac{\sqrt{110}}{5}+\frac{4\sqrt{42}}{21}+\frac{\sqrt{30}}{3}+\frac{2\sqrt{3}}{7}-\frac{10}{9}+8m\right)n.
\end{aligned} \tag{11}$$

4.5. The Geometric-Arithmetic Index Developed by ve-Degree Methodology. Utilizing the edge-partition details described in the Table 2, we measured the geometric-arithmetic index developed by *ve*-degree methodology:

$$\begin{aligned}
GA_{ve}\left(Y_m^1(n,n)\right) &= \sum_{x_1x_2\in E}\frac{2\left(\xi_{ve}(x_1)\times\xi_{ve}(x_2)\right)^{(1/2)}}{\xi_{ve}(x_1)+\xi_{ve}(x_2)} \\
&= (2n)\frac{(2)\sqrt{25}}{10}+(4n)\frac{(2)\sqrt{40}}{13}+(2n)\frac{(2)\sqrt{63}}{16}+(2n)\frac{(2)\sqrt{21}}{10} \\
&\quad +(4n)\frac{(2)\sqrt{72}}{17}+(n)\frac{(2)\sqrt{49}}{14}+\frac{(2)\sqrt{81}}{18}\left(\frac{9n^2}{4}-\frac{5n}{2}+18mn+9\right) \\
&= 9+\frac{9n^2}{4}+\left(\frac{1}{2}+\frac{16\sqrt{10}}{13}+\frac{3\sqrt{7}}{4}+\frac{2\sqrt{21}}{5}+\frac{48\sqrt{2}}{17}+18m\right)n.
\end{aligned} \tag{12}$$

4.6. The Harmonic Index Developed by ve-Degree Methodology. Utilizing the edge-partition details described in the Table 2, we measured the harmonic index developed by *ve*-degree methodology:

$$\begin{aligned}
H_{ve}\left(Y_m^1(n,n)\right) &= \sum_{x_1x_2\in E}\frac{2}{\xi_{ve}(x_1)+\xi_{ve}(x_2)} \\
&= (2n)\frac{2}{10}+(4n)\frac{2}{13}+(2n)\frac{2}{16}+(2n)\frac{2}{10}+(4n)\frac{2}{17}+(n)\frac{2}{14}+\frac{2}{18}\left(\frac{9n^2}{4}-\frac{5n}{2}+18mn+9\right) \\
&= 1+\frac{n^2}{4}+\left(\frac{557213}{278460}+2m\right)n.
\end{aligned} \tag{13}$$

4.7. The Sum-Connectivity Index Developed by ve-Degree Methodology. Utilizing the edge-partition details described in the Table 2, we measured the sum-connectivity index developed by *ve*-degree methodology:

$$\begin{aligned}
\chi_{ve}\left(Y_m^1(n,n)\right) &= \sum_{x_1x_2\in E}\left(\xi_{ve}(x_1)+\xi_{ve}(x_2)\right)^{(-1/2)} \\
&= (2n)\frac{1}{\sqrt{10}}+(4n)\frac{1}{\sqrt{13}}+(2n)\frac{1}{\sqrt{16}}+(2n)\frac{1}{\sqrt{10}}+(4n)\frac{1}{\sqrt{17}}+(n)\frac{1}{\sqrt{14}}+\frac{1}{\sqrt{18}}\left(\frac{9n^2}{4}-\frac{5n}{2}+18mn+9\right) \\
&= \left(\frac{2\sqrt{10}}{5}+\frac{4\sqrt{13}}{13}+\frac{1}{2}+\frac{4\sqrt{17}}{17}+\frac{\sqrt{14}}{14}+\frac{\sqrt{2}}{6}\left(\frac{-5}{2}+18m\right)\right)n+\frac{3\sqrt{2}n^2}{8}+\frac{3\sqrt{2}}{2}.
\end{aligned} \tag{14}$$

5. The *ve*-Degree Results of *Y*-Junction Graph $Y_m^2(n,n)$

By attaching the $4n$ pendants vertices with 2 degree vertices to any two tube of $Y_m(n,n)$ graph, we obtain a new graph, it is denoted by $Y_m^2(n,n)$, see Figure 3. The cardinality of $Y_m^2(n,n)$ is $(3n^2/2)+13n+12mn+6$ and size is $(9n^2/4)+(29n/2)+18mn+9$. This section determined the *ve*-degree results of *Y*-junction graph $Y_m^2(n,n)$. The edge partition of end vertices *ve*-degree of each edge along with the degree of end vertices of each edge for $Y_m^2(n,n)$ graph is given in Table 3.

5.1. The First ve-Degree Zagreb β Index.

$$\begin{aligned} M_{\beta ve}^1\left(Y_m^2(n,n)\right) &= \sum_{x_1x_2\in E}\left(\xi_{ve}(x_1)+\xi_{ve}(x_2)\right)\\ &= (10)(n)+(13)(2n)+(16)(4n)+(10)(4n)+(17)(2n)+(14)(2n)+(18)\left(\frac{9n^2}{4}-\frac{n}{2}+18mn+9\right)\\ &= 162+\frac{81n^2}{2}+(193+324m)n. \end{aligned} \tag{15}$$

5.2. The Second Zagreb Index Developed by ve-Degree Methodology.

$$\begin{aligned} M_{ve}^2\left(Y_m^2(n,n)\right) &= \sum_{x_1x_2\in E}\left(\xi_{ve}(x_1)\times\xi_{ve}(x_2)\right)\\ &= (25)(n)+(40)(2n)+(63)(4n)+(21)(4n)+(72)(2n)+(49)(2n)+(81)\left(\frac{9n^2}{4}-\frac{n}{2}+18mn+9\right)\\ &= 729+\frac{729n^2}{4}+\left(\frac{1285}{2}+1458m\right)n. \end{aligned} \tag{16}$$

5.3. The Randić Index Developed by ve-Degree Methodology. Utilizing the edge-partition details described in the Table 3, we measured the Randić index developed by *ve*-degree methodology:

$$\begin{aligned} R_{ve}\left(Y_m^2(n,n)\right) &= \sum_{x_1x_2\in E}\left(\xi_{ve}(x_1)\times\xi_{ve}(x_2)\right)^{(-1/2)}\\ &= (35)^{(-1/2)}(n)+(40)^{(-1/2)}(2n)+(63)^{(-1/2)}(4n)+(21)^{(-1/2)}(4n)\\ &\quad+(72)^{(-1/2)}(2n)+(49)^{(-1/2)}(2n)+(81)^{(-1/2)}\left(\frac{9n^2}{4}-\frac{n}{2}+18mn+9\right)\\ &= 1+\frac{n^2}{4}+\left(\frac{271}{630}+\frac{\sqrt{10}}{10}+\frac{4\sqrt{7}}{21}+\frac{4\sqrt{21}}{21}+\frac{\sqrt{2}}{6}+2m\right)n. \end{aligned} \tag{17}$$

5.4. The Atom-Bond Connectivity Index Developed by ve-Degree Methodology. Utilizing the edge-partition details described in the Table 3, we measured the atom-bond connectivity index developed by *ve*-degree methodology:

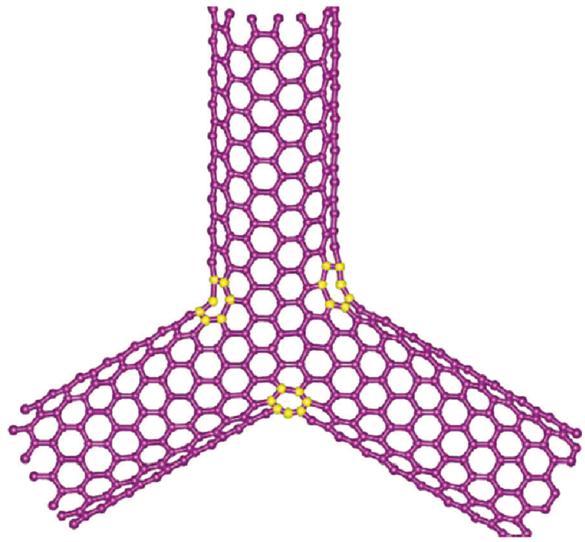

Figure 3: A variant of Y-junction $Y_m^2(n,n)$.

Table 3: The ve-degrees of each edge of $Y_m^2(n,n)$.

$(\xi(x_1),\xi(x_2))$	$(\xi_{ve}(x_1),\xi_{ve}(x_2))$	Count
$(2,2)$	$(5,5)$	n
$(2,3)$	$(5,8)$	$2n$
$(3,3)$	$(7,9)$	$4n$
$(1,3)$	$(3,7)$	$4n$
$(2,3)$	$(8,9)$	$2n$
$(3,3)$	$(7,7)$	$2n$
$(3,3)$	$(9,9)$	$(9n^2/4)-(n/2)+18mn+9$

$$\begin{aligned}
ABC_{ve}\left(Y_m^2(n,n)\right) &= \sum_{x_1x_2\in E}\left(\frac{\xi_{ve}(x_1)+\xi_{ve}(x_2)-2}{\xi_{ve}(x_1)\times\xi_{ve}(x_2)}\right)^{(1/2)}\\
&= (n)\sqrt{\frac{8}{25}}+(2n)\sqrt{\frac{11}{40}}+(4n)\sqrt{\frac{14}{63}}+(4n)\sqrt{\frac{8}{21}}+(2n)\sqrt{\frac{15}{72}}+(2n)\sqrt{\frac{12}{49}}+\sqrt{\frac{16}{81}}\left(\frac{9n^2}{4}-\frac{n}{2}+18mn+9\right)\\
&= 4+n^2+\left(\frac{26\sqrt{2}}{15}+\frac{\sqrt{110}}{10}+\frac{8\sqrt{42}}{21}+\frac{\sqrt{30}}{6}+\frac{4\sqrt{3}}{7}-\frac{2}{9}+8m\right)n.
\end{aligned} \tag{18}$$

5.5. The Geometric-Arithmetic Index Developed by ve-Degree Methodology. Utilizing the edge-partition details described in the Table 3, we measured the geometric-arithmetic index developed by ve-degree methodology:

$$\begin{aligned}
GA_{ve}\left(Y_m^2(n,n)\right) &= \sum_{x_1x_2\in E}\frac{2\left(\xi_{ve}(x_1)\times\xi_{ve}(x_2)\right)^{(1/2)}}{\xi_{ve}(x_1)+\xi_{ve}(x_2)}\\
&= (n)\frac{(2)\sqrt{25}}{10}+(2n)\frac{(2)\sqrt{40}}{13}+(4n)\frac{(2)\sqrt{63}}{16}+(4n)\frac{(2)\sqrt{21}}{10}+(2n)\frac{(2)\sqrt{72}}{17}\\
&\quad+(2n)\frac{(2)\sqrt{49}}{14}+\frac{(2)\sqrt{81}}{18}\left(\frac{9n^2}{4}-\frac{n}{2}+18mn+9\right)\\
&= 9+\frac{9n^2}{4}+\left(\frac{5}{2}+\frac{8\sqrt{10}}{13}+\frac{3\sqrt{7}}{2}+\frac{4\sqrt{21}}{5}+\frac{24\sqrt{2}}{17}+18m\right)n.
\end{aligned} \tag{19}$$

5.6. The Harmonic Index Developed by ve-Degree Methodology. Utilizing the edge-partition details described in the Table 3, we measured the harmonic index developed by *ve*-degree methodology:

$$\begin{aligned}H_{ve}\left(Y_m^2(n,n)\right) &= \sum_{x_1x_2\in E}\frac{2}{\xi_{ve}(x_1)+\xi_{ve}(x_2)}\\ &= (n)\frac{2}{10}+(2n)\frac{2}{13}+(4n)\frac{2}{16}+(4n)\frac{2}{10}+(2n)\frac{2}{17}+(2n)\frac{2}{14}+\frac{2}{18}\left(\frac{9n^2}{4}-\frac{n}{2}+18mn+9\right)\\ &= 1+\frac{n^2}{4}+\left(\frac{31649}{13923}+2m\right)n.\end{aligned}\tag{20}$$

5.7. The Sum-Connectivity Index Developed by ve-Degree Methodology. Utilizing the edge-partition details described in the Table 3, we measured the sum-connectivity index developed by *ve*-degree methodology:

$$\begin{aligned}\chi_{ve}\left(Y_m^2(n,n)\right) &= \sum_{x_1x_2\in E}\left(\xi_{ve}(x_1)+\xi_{ve}(x_2)\right)^{(-1/2)}\\ &= (n)\frac{1}{\sqrt{10}}+(2n)\frac{1}{\sqrt{13}}+(4n)\frac{1}{\sqrt{16}}+(4n)\frac{1}{\sqrt{10}}+(2n)\frac{1}{\sqrt{17}}+(2n)\frac{1}{\sqrt{14}}+\frac{1}{\sqrt{18}}\left(\frac{9n^2}{4}-\frac{n}{2}+18mn+9\right)\\ &= \left(\frac{\sqrt{10}}{2}+\frac{2\sqrt{13}}{13}+1+\frac{2\sqrt{17}}{17}+\frac{\sqrt{14}}{7}+\frac{\sqrt{2}}{6}\left(-\frac{1}{2}+18m\right)\right)n+\frac{3\sqrt{2}n^2}{8}+\frac{3\sqrt{2}}{2}.\end{aligned}\tag{21}$$

6. The *ve*-Degree Results of *Y*-Junction Graph $Y_m^3(n,n)$

In $Y_m(n,n)$ when one tube appears with exactly $2n$ pendants, we denote it by $Y_m^1(n,n)$, see Figure 2. The order and size of this new graph is $(3n^2/2)+11n+12mn+6$ and $(9n^2/4)+(25n/2)+18mn+9$, respectively. The Y-junction graph $Y_m^2(n,n)$ is obtained by attaching $4n$ pendants to any two tubes of $Y_m(n,n)$, see Figure 3. The cardinality of $Y_m^2(n,n)$ is $(3n^2/2)+13n+12mn+6$ and size is $(9n^2/4)+(29n/2)+18mn+9$. The graph $Y_m(n,n)$ with maximum possible pendants denoted by $Y_m^3(n,n)$, see Figure 4. It has order $(3n^2/2)+15n+12mn+6$ and size $(9n^2/4)+(33n/2)+18mn+9$.

6.1. The First ve-Degree Zagreb β Index.

$$\begin{aligned}M_{\beta ve}^1\left(Y_m^3(n,n)\right) &= \sum_{x_1x_2\in E}\left(\xi_{ve}(x_1)+\xi_{ve}(x_2)\right)\\ &= (16)(6n)+(10)(6n)+(14)(3n)\\ &\quad+(18)\left(\frac{9n^2}{4}+\frac{3n}{2}+18mn+9\right)\\ &= 162+\frac{81n^2}{2}+(225+324m)n.\end{aligned}\tag{22}$$

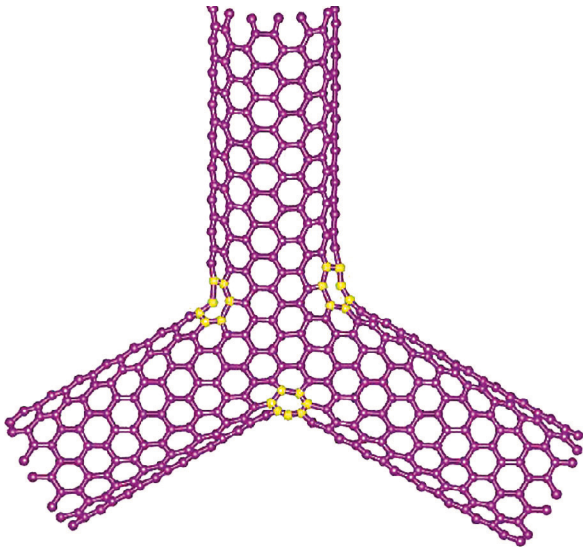

Figure 4: A variant of Y-junction $Y_m^3(n,n)$.

6.2. The Second Zagreb Index Developed by ve-Degree Methodology.

$$\begin{aligned} M_{ve}^2\left(Y_m^3(n,n)\right) &= \sum_{x_1x_2\in E} \left(\xi_{ve}(x_1)\times\xi_{ve}(x_2)\right) \\ &= (63)(6n)+(21)(6n)+(49)(3n) \\ &\quad +(81)\left(\frac{9n^2}{4}+\frac{3n}{2}+18mn+9\right) \\ &= 729+\frac{729n^2}{4}+\left(\frac{1545}{2}+1458m\right)n. \end{aligned} \tag{23}$$

6.3. The Randić Index Developed by ve-Degree Methodology. Utilizing the edge-partition details described in the Table 4, we measured the Randić index developed by *ve*-degree methodology:

$$\begin{aligned} R_{ve}\left(Y_m^3(n,n)\right) &= \sum_{x_1x_2\in E} \left(\xi_{ve}(x_1)\times\xi_{ve}(x_2)\right)^{(-1/2)} \\ &= (63)^{(-1/2)}(6n)+(21)^{(-1/2)}(6n)+(49)^{(-1/2)}(3n) \\ &\quad +(81)^{(-1/2)}\left(\frac{9n^2}{4}+\frac{3n}{2}+18mn+9\right) \\ &= 1+\frac{n^2}{4}+\left(\frac{2\sqrt{7}}{7}+\frac{2\sqrt{21}}{7}+\frac{25}{42}+2m\right)n. \end{aligned} \tag{24}$$

6.4. The Atom-Bond Connectivity Index Developed by ve-Degree Methodology. Utilizing the edge-partition details described in the Table 4, we measured the atom-bond connectivity index developed by *ve*-degree methodology:

$$\begin{aligned} ABC_{ve}\left(Y_m^3(n,n)\right) &= \sum_{x_1x_2\in E} \left(\frac{\xi_{ve}(x_1)+\xi_{ve}(x_2)-2}{\xi_{ve}(x_1)\times\xi_{ve}(x_2)}\right)^{(1/2)} \\ &= (6n)\sqrt{\frac{14}{63}}+(6n)\sqrt{\frac{8}{21}}+(3n)\sqrt{\frac{12}{49}}+\sqrt{\frac{16}{81}}\left(\frac{9n^2}{4}+\frac{3n}{2}+18mn+9\right) \\ &= 4+n^2+\left(2\sqrt{2}+\frac{4\sqrt{42}}{7}+\frac{6\sqrt{3}}{7}+\frac{2}{3}+8m\right)n. \end{aligned} \tag{25}$$

6.5. The Geometric-Arithmetic Index Developed by ve-Degree Methodology. Utilizing the edge-partition details described in the Table 4, we measured the geometric-arithmetic index developed by *ve*-degree methodology:

Table 4: The ve-degrees of each edge of $Y_m^3(n,n)$.

$(\xi(x_1),\xi(x_2))$	$(\xi_{ve}(x_1),\xi_{ve}(x_2))$	Count
$(3,3)$	$(7,9)$	$6n$
$(1,3)$	$(3,7)$	$6n$
$(3,3)$	$(7,7)$	$3n$
$(3,3)$	$(9,9)$	$(9n^2/4)-(3n/2)+18mn+9$

Table 5: Numerical comparison of $M^1_{\beta ve}$, M^2_{ve}, H_{ve}, R_{ve}, χ_{ve}, ABC_{ve}, GA_{ve} for Y-junction graph $Y_m(n,n)$.

(m,n)	$M^1_{\beta ve}$	M^2_{ve}	R_{ve}	ABC_{ve}	GA_{ve}	H_{ve}	χ_{ve}
(5, 5)	9919.50	43647.8	66.0289	256.910	566.888	65.8948	136.481
(6, 6)	14058.0	62073.0	92.5347	361.493	799.966	92.3738	191.992
(7, 7)	18925.5	83778.8	123.541	484.074	1073.55	123.353	257.048
(8, 8)	24522.0	108765.0	159.046	624.656	1387.62	158.832	331.649
(9, 9)	30847.5	137032.0	199.052	783.240	1742.20	198.811	415.797
(10, 10)	37902.0	168579.0	243.558	959.820	2137.28	243.290	509.491
(11, 11)	45685.5	203407.0	292.564	1154.40	2572.86	292.269	612.730
(12, 12)	54198.0	241515.0	346.069	1366.98	3048.94	345.748	725.515
(13, 13)	63439.5	282904.0	404.075	1597.56	3565.50	403.726	847.847
(14, 14)	73410.0	327573.0	466.581	1846.15	4122.58	466.205	979.724

Table 6: Numerical comparison of $M^1_{\beta ve}$, M^2_{ve}, H_{ve}, R_{ve}, χ_{ve}, ABC_{ve}, GA_{ve} for Y-junction graph $Y^1_m(n,n)$.

(m,n)	$M^1_{\beta ve}$	M^2_{ve}	R_{ve}	ABC_{ve}	GA_{ve}	H_{ve}	χ_{ve}
(5, 5)	10079.5	44297.8	67.5368	262.078	576.262	67.2553	139.058
(6, 6)	14250.0	62853.0	94.3441	367.695	811.214	94.0063	195.082
(7, 7)	19149.5	84688.8	125.652	491.309	1086.66	125.257	260.653
(8, 8)	24778.0	109805.0	161.459	632.925	1402.61	161.008	335.770
(9, 9)	31135.5	138202.0	201.767	792.543	1759.08	201.259	420.433
(10, 10)	38222.0	169879.0	246.574	970.157	2156.02	246.011	514.641
(11, 11)	46037.5	204837.0	295.881	1165.77	2593.47	295.262	618.397
(12, 12)	54582.0	243075.0	349.688	1379.39	3071.43	349.013	731.697
(13, 13)	63855.5	284594.0	407.996	1611.0	3589.89	407.264	854.543
(14, 14)	73858.0	329393.0	470.803	1860.62	4148.83	470.015	986.937

$$\begin{aligned}
GA_{ve}\left(Y_m^3(n,n)\right) &= \sum_{x_1x_2\in E}\frac{2\left(\xi_{ve}(x_1)\times\xi_{ve}(x_2)\right)^{1/2}}{\xi_{ve}(x_1)+\xi_{ve}(x_2)}\\
&= (6n)\frac{(2)\sqrt{63}}{16}+(6n)\frac{(2)\sqrt{21}}{10}+(3n)\frac{(2)\sqrt{49}}{14}+\frac{(2)\sqrt{81}}{18}\left(\frac{9n^2}{4}+\frac{3n}{2}+18mn+9\right)\\
&= 9+\frac{9n^2}{4}+\left(\frac{9\sqrt{7}}{4}+\frac{6\sqrt{21}}{5}+\frac{9}{2}+18m\right)n.
\end{aligned}\tag{26}$$

6.6. The Harmonic Index Developed by ve-Degree Methodology. Utilizing the edge-partition details described in the Table 4, we measured the harmonic index developed by ve-degree methodology:

TABLE 7: Numerical comparison of $M^1_{\beta ve}$, M^2_{ve}, H_{ve}, R_{ve}, χ_{ve}, ABC_{ve}, GA_{ve} for Y-junction graph $Y^2_m(n,n)$.

(m,n)	$M^1_{\beta ve}$	M^2_{ve}	R_{ve}	ABC_{ve}	GA_{ve}	H_{ve}	χ_{ve}
(5, 5)	10239.5	44947.8	69.0446	267.247	585.636	68.6157	141.634
(6, 6)	14442.0	63633.0	96.1536	373.896	822.463	95.6389	198.173
(7, 7)	19373.5	85598.8	127.763	498.545	1099.79	127.162	264.260
(8, 8)	25034.0	110845.0	163.872	641.194	1417.62	163.185	339.891
(9, 9)	31423.5	139372.0	204.480	801.845	1775.94	203.708	425.069
(10, 10)	38542.0	171179.0	249.590	980.494	2174.78	248.731	519.793
(11, 11)	46389.5	206267.0	299.199	1177.15	2614.10	298.255	624.062
(12, 12)	54966.0	244635.0	353.306	1391.80	3093.92	352.278	737.878
(13, 13)	64271.5	286284.0	411.915	1624.45	3614.25	410.801	861.241
(14, 14)	74306.0	331213.0	475.024	1875.09	4175.07	473.824	994.147

TABLE 8: Numerical comparison of $M^1_{\beta ve}$, M^2_{ve}, H_{ve}, R_{ve}, χ_{ve}, ABC_{ve}, GA_{ve} for Y-junction graph $Y^3_m(n,n)$.

(m,n)	$M^1_{\beta ve}$	M^2_{ve}	R_{ve}	ABC_{ve}	GA_{ve}	H_{ve}	χ_{ve}
(5, 5)	10399.5	45597.8	70.5523	272.414	595.010	69.9762	144.209
(6, 6)	14634.0	64413.0	97.9629	380.098	833.713	97.2714	201.264
(7, 7)	19597.5	86508.8	129.873	505.781	1112.91	129.067	267.865
(8, 8)	25290.0	111885.0	166.283	649.463	1432.61	165.362	344.012
(9, 9)	31711.5	140542.0	207.194	811.148	1792.82	206.157	429.705
(10, 10)	38862.0	172479.0	252.604	990.830	2193.52	251.452	524.945
(11, 11)	46741.5	207697.0	302.515	1188.51	2634.72	301.248	629.729
(12, 12)	55350.0	246195.0	356.926	1404.20	3116.43	355.543	744.059
(13, 13)	64687.5	287974.0	415.836	1637.88	3638.63	414.338	867.937
(14, 14)	74754.0	333033.0	479.246	1889.56	4201.33	477.633	1001.36

$$
\begin{aligned}
H_{ve}\left(Y^3_m(n,n)\right) &= \sum_{x_1x_2\in E} \frac{2}{\xi_{ve}(x_1)+\xi_{ve}(x_2)}\\
&= (6n)\frac{2}{16} + (6n)\frac{2}{10}\\
&\quad + (3n)\frac{2}{14} + \frac{2}{18}\left(\frac{9n^2}{4} + \frac{3n}{2} + 18mn + 9\right)\\
&= 1 + \frac{n^2}{4} + \left(\frac{1069}{420} + 2m\right)n.
\end{aligned}
\tag{27}
$$

6.7. The Sum-Connectivity Index Developed by ve-Degree Methodology. Utilizing the edge-partition details described in the Table 4, we measured the sum-connectivity index developed by *ve*-degree methodology:

$$
\begin{aligned}
\chi_{ve}\left(Y^3_m(n,n)\right) &= \sum_{x_1x_2\in E} \left(\xi_{ve}(x_1)+\xi_{ve}(x_2)\right)^{(-1/2)}\\
&= (6n)\frac{1}{\sqrt{16}} + (6n)\frac{1}{\sqrt{10}} + (3n)\frac{1}{\sqrt{14}} + \frac{1}{\sqrt{18}}\left(\frac{9n^2}{4} + \frac{3n}{2} + 18mn + 9\right)\\
&= \frac{3\sqrt{2}n^2}{8} + \left(\frac{3}{2} + \frac{3\sqrt{10}}{5} + \frac{3\sqrt{14}}{14} + \frac{\sqrt{2}}{6}\left(\frac{3}{2} + 18m\right)\right)n + \frac{3\sqrt{2}}{2}.
\end{aligned}
\tag{28}
$$

7. Conclusion

In this research work, *ve*-degree topological indices are measured of Y-junctions and their three different variants. We determined the first *ve*-degree Zagreb β-index, second Zagreb index, Randić, atom-bond-connectivity index, general sum-connectivity and geometric-arithmetic, and harmonic index developed by *ve*-degree methodology, for four types of Y-shaped carbon nanotube junctions $Y_m(n,n)$. The results of Y-junctions and their structures also are elaborated in numerical Tables 5–8. Instead of a whole complex structure, it will be easy to see as a numeric quantity.

Data Availability

There is not data associative with this manuscript.

Conflicts of Interest

The author declares that he has no conflicts of interest.

Acknowledgments

There is no Funding associative with this manuscript.

References

[1] M. Chellali, T. W. Haynes, S. T. Hedetniemi, and T. M. Lewis, "On ve-degrees and ev-degrees in graphs," *Discrete Mathematics*, vol. 340, no. 2, pp. 31–38, 2017.

[2] A. Ahmad, "Comparative study of ve-degree and ev-degree topological descriptors for benzene ring embedded in p-type-surface in 2D network," *Polycyclic Aromatic Compounds*, 2020.

[3] A.-N. A.-H. Ahmad, A. Ahmad, and M. Azeem, "Computation of edge- and vertex-degree-based topological indices for tetrahedral sheets of clay minerals," *Main Group Metal Chemistry*, vol. 45, no. 1, pp. 26–34, 2022.

[4] B. Horoldagva, K. C. Das, and T.-A. Selenge, "On ve-degree and ev-degree of graphs," *Discrete Optimization*, vol. 31, pp. 1–7, 2019.

[5] S. Ediz, "On ve-degree molecular topological properties of silicate and oxygen networks," *International Journal of Computing Science and Mathematics*, vol. 9, no. 1, pp. 1–12, 2018.

[6] B. Sahin and S. Ediz, "On ev-degree and ve-degree topological indices, Iran," *Journal of Mathematical Chemistry*, vol. 9, no. 4, pp. 263–277, 2018.

[7] M. F. Nadeem, A. Shabbir, and M. Azeem, "On metric dimension and fault tolerant metric dimension of some chemical structures," *Polycyclic Aromatic Compounds*, 2021.

[8] M. F. Nadeem, M. Hassan, M. Azeem et al., "Application of resolvability technique to investigate the different polyphenyl structures for polymer industry," *Journal of Chemistry*, vol. 2021, Article ID 6633227, 8 pages, 2021.

[9] A. Aiyiti, Z. Zhang, B. Chen et al., "Thermal rectification in *Y*-junction carbon nanotube bundle," *Carbon*, vol. 140, pp. 673–679, 2018.

[10] D.-H. Kim, J. Huang, H.-K. Shin, S. Roy, and W. Choi, "Transport phenomena and conduction mechanism of single-walled carbon nanotubes (SWNTs) at *Y*- and crossed-junctions," *Nano Letters*, vol. 6, no. 12, pp. 2821–2825, 2006.

[11] H. Mei and Y. Cheng, "Research progress of electrical properties based on carbon nanotubes; interconnection," *Ferroelectrics*, vol. 564, no. 1, 2020.

[12] V. Meunier, M. B. Nardelli, J. Bernholc, T. Zacharia, and J.-C. Charlier, "Intrinsic electron transport properties of carbon nanotube *Y*-junctions," *Applied Physics Letters*, vol. 81, no. 27, pp. 5234–5236, 2002.

[13] S. Hayat and M. Imran, "Computation of topological indices of certain networks," *Applied Mathematics and Computation*, vol. 240, pp. 213–228, 2014.

[14] N. A. Koam and A. Ahmad, "Polynomials of degree-based indices for three-dimensional mesh network," *Computers, Materials and Continua*, vol. 65, no. 2, pp. 1271–1282, 2020.

[15] M. Javaid, J.-B. Liu, M. A. Rehman, and S. Wang, "On the certain topological indices of titania nanotube TiO_2 [m, n]," *Zeitschrift für Naturforschung A*, vol. 72, no. 7, pp. 647–654, 2017.

[16] A. Aslam, Y. Bashir, S. Ahmad, and W. Gao, "On topological indices of certain dendrimer structures," *Zeitschrift für Naturforschung A*, vol. 72, no. 6, pp. 559–566, 2017.

[17] G. Hong, Z. Gu, M. Javaid, H. M. Awais, and M. K. Siddiqui, "Degree-based topological invariants of metal-organic networks," *IEEE Access*, vol. 8, pp. 68288–68300, 2020.

[18] H. M. Afzal Siddiqui, M. F. Nadeem, M. Azeem, M. A. Arshad, A. Haider, and M. A. Malik, "Topological properties of supramolecular chain of different complexes of N-salicylidene-L-valine," *Polycyclic Aromatic Compounds*, 2021.

[19] X. Zuo, M. F. Nadeem, M. K. Siddiqui, and M. Azeem, "Edge weight based entropy of different topologies of carbon nanotubes," *IEEE Access*, vol. 9, pp. 102019–102029, 2021.

[20] M. F. Nadeem, M. Imran, H. M. Afzal Siddiqui, M. Azeem, A. Khalil, and Y. Ali, "Topological aspects of metal-organic structure with the help of underlying networks," *Arabian Journal of Chemistry*, vol. 14, no. 6, Article ID 103157, 2021.

[21] A. Ahmad, R. Hasni, N. Akhter, and K. Elahi, "Analysis of distance-based topological polynomials associated with zero-divisor graphs," *Computers, Materials and Continua*, vol. 70, no. 2, pp. 2895–2904, 2022.

[22] M. K. Siddiqui, M. Imran, and A. Ahmad, "On zagreb indices, zagreb polynomials of some nanostar dendrimers," *Applied Mathematics and Computation*, vol. 280, pp. 132–139, 2016.

[23] H. Yang, A. Q. Baig, W. Khalid, M. R. Farahani, and X. Zhang, "M-Polynomial and topological indices of benzene ring embedded in p-type surface network," *Journal of Chemistry*, vol. 2019, Article ID 7297253, 9 pages, 2019.

[24] Z. Shao, M. Siddiqui, and M. Muhammad, "Computing zagreb indices and zagreb polynomials for symmetrical nanotubes," *Symmetry*, vol. 10, no. 7, p. 244, 2018.

[25] W. Gao, M. Asif, and W. Nazeer, "The study of honey comb derived network via topological indices," *Open Journal of Mathematical Analysis*, vol. 2, pp. 10–26, 2018.

[26] H. Raza, M. Waheed, M. K. Jamil, and M. Azeem, "Structures devised by the generalizations of two graph operations and their topological descriptors," *Main Group Metal Chemistry*, vol. 45, no. 1, pp. 44–56, 2022.

[27] G. Abbas, M. Ibrahim, A. Ahmad, M. Azeem, and K. Elahi, "M-polynomials of tetra-cyano-benzene transition metal structure," *Polycyclic Aromatic Compounds*, 2021.

[28] M. Cancan, "On ev-degree and ve-degree topological properties of tickysim spiking neural network," *Computational Intelligence and Neuroscience*, vol. 2019, Article ID 8429120, 7 pages, 2019.

[29] H. Deng, J. Yang, and F. Xia, "A general modeling of some vertex-degree based topological indices in benzenoid systems and phenylenes," *Computers and Mathematics with Applications*, vol. 61, no. 10, pp. 3017–3023, 2011.

[30] J. Zhang, M. K. Siddiqui, A. Rauf, and M. Ishtiaq, "On ve-degree and ev-degree based topological properties of single walled titanium dioxide nanotube," *Journal of Cluster Science*, vol. 32, 2020.

[31] A. Ahmad and A. N. Koam, "Computing the topological descriptors of line graph of the complete m-ary trees," *Journal of Intelligent and Fuzzy Systems*, vol. 39, no. 1, pp. 1081–1088, 2020.

[32] W. Gao, M. Siddiqui, M. Naeem, and N. Rehman, "Topological characterization of carbon graphite and crystal cubic carbon structures," *Molecules*, vol. 22, no. 9, p. 1496, 2017.

[33] A. Ahmad, "Topological properties of sodium chloride," *UPB Scientific Bulletin, Series B*, vol. 82, no. 1, pp. 35–46, 2020.

[34] Y. Shi, "Note on two generalizations of the randić index," *Applied Mathematics and Computation*, vol. 265, pp. 1019–1025, 2015.

[35] M. Bača, J. Horváthová, M. Mokrišová, and A. Suhányiová, "On topological indices of fullerenes," *Applied Mathematics and Computation*, vol. 251, pp. 154–161, 2015.

[36] A. Ahmad, "On the degree based topological indices of benzene ring embedded in P-type-surface in 2D network," *Hacettepe Journal of Mathematics and Statistics*, vol. 4, no. 46, pp. 9–18, 2017.

[37] A. Ahmad, K. Elahi, R. Hasni, and M. F. Nadeem, "Computing the degree based topological indices of line graph of benzene ring embedded in P-type-surface in 2D network," *Journal of Information and Optimization Sciences*, vol. 40, no. 7, pp. 1511–1528, 2019.

[38] K. Nagy and C. L. Nagy, "Hypergraphene from armchair nanotube *Y* junctions," *Diamond and Related Nanostructures*, vol. 6, pp. 207–227, 2013.

[39] M. F. Nadeem and A. Shabbir, "Computing and comparative analysis of topological invariants of *Y*-junction carbon nanotubes," *International Journal of Quantum Chemistry*, vol. 122, no. 5, 2021.

[40] M. V. Diudea, *Nanostructures, Novel Architecture*, NOVA, New York, NY, USA, 2005.

[41] M. V. Diudea and C. L. Nagy, *Periodic Nanostructures*, Springer, Dordrecht, Netherlands, 2007.